



Long-range transport of black carbon to the Pacific Ocean

J. Zhang et al.

Long-range transport of black carbon to the Pacific Ocean and its dependence on aging timescale

J. Zhang^{1,2,3}, J. Liu¹, S. Tao¹, and G. A. Ban-Weiss³

¹Laboratory for Earth Surface Processes, College of Urban and Environmental Sciences, Peking University, Beijing, China

²School of Physics, Peking University, Beijing, China

³Department of Civil and Environmental Engineering, University of Southern Los Angeles, CA, USA

Received: 22 May 2015 – Accepted: 03 June 2015 – Published: 22 June 2015

Correspondence to: J. Liu (jliu@pku.edu.cn)

Published by Copernicus Publications on behalf of the European Geosciences Union.

Title Page

Abstract

Introduction

Conclusions

References

Tables

Figures



Back

Close

Full Screen / Esc

Printer-friendly Version

Interactive Discussion



Abstract

Improving the ability of global models to predict concentrations of black carbon (BC) over the Pacific Ocean is essential to evaluate the impact of BC on marine climate. In this study, we tag BC tracers from 13 source regions around the globe in a global chemical transport model MOZART-4. Numerous sensitivity simulations are carried out varying the aging timescale of BC emitted from each source region. The aging timescale for each source region is optimized by minimizing errors in vertical profiles of BC mass mixing ratios between simulations and HIAPER Pole-to-Pole Observations (HIPPO). For most HIPPO deployments, in the Northern Hemisphere, optimized aging timescales are less than half a day for BC emitted from tropical and mid-latitude source regions, and about 1 week for BC emitted from high latitude regions in all seasons except summer. We find that East Asian emissions contribute most to the BC loading over the North Pacific, while South American, African and Australian emissions dominate BC loadings over the South Pacific. Dominant source regions contributing to BC loadings in other parts of the globe are also assessed. The lifetime of BC originating from East Asia (i.e., the world's largest BC emitter) is found to be only 2.2 days, much shorter than the global average lifetime of 4.9 days, making East Asia's contribution to global burden only 36 % of BC from the second largest emitter, Africa. Thus, evaluating only relative emission rates without accounting for differences in aging timescales and deposition rates is not predictive of the contribution of a given source region to climate impacts. Our simulations indicate that lifetime of BC increases nearly linearly with aging timescale for all source regions. When aging rate is fast, the lifetime of BC is largely determined by factors that control local deposition rates (e.g. precipitation). The sensitivity of lifetime to aging timescale depends strongly on the initial hygroscopicity of freshly emitted BC. Our findings suggest that the aging timescale of BC varies significantly by region and season, and can strongly influence the contribution of source regions to BC burdens around the globe. Improving parameterizations of the aging process for BC is important for enhancing the predictive skill of air quality and climate

Long-range transport of black carbon to the Pacific Ocean

J. Zhang et al.

Title Page

Abstract

Introduction

Conclusions

References

Tables

Figures



Back

Close

Full Screen / Esc

Printer-friendly Version

Interactive Discussion



models. Future observations that investigate the evolution of hygroscopicity of BC as it ages from different source regions to the remote atmosphere are urgently needed.

1 Introduction

Black carbon (BC) is an efficient absorber of solar radiation and therefore heats the atmosphere and the Earth surface (Ramanathan and Carmichael, 2008). Estimates of BC's direct radiative forcing widely vary, ranging from 0.19 W m^{-2} by Wang et al. (2014) to 0.88 W m^{-2} by Bond et al. (2013). The Intergovernmental Panel on Climate Change Fifth Assessment Report (IPCC AR5) assesses the direct radiative forcing of BC to be 0.40 W m^{-2} with a large uncertainty range of 0.05 to 0.80 W m^{-2} . Besides its direct radiative effects, BC also affects Earth's energy budget indirectly by influencing cloud formation (Koch and Del Genio, 2010) and snow albedo (Hansen and Nazarenko, 2004; Flanner et al., 2007; He et al., 2014), although these processes are relatively less understood and subject to greater uncertainties. In addition, epidemiological studies have shown that BC is associated with increased hospital admissions and premature mortalities (Bell et al., 2009; Janssen et al., 2011).

Relative to greenhouse gases, BC has a shorter lifetime, and its concentration changes considerably by location and season (Liu et al., 2011). Horizontal and vertical distributions of BC are not well constrained with observations, contributing to the uncertainties in estimates of BC's radiative forcing (Bond et al., 2013). BC has higher radiative forcing efficiency (i.e. radiative forcing per unit mass of BC) when its underlying surface is highly reflective (e.g. cloud, snow and ice). The radiative forcing of BC also depends on its altitude, and is enhanced if located above clouds relative to below clouds (Satheesh, 2002; Zarzycki and Bond, 2010). The direct radiative forcing efficiency of BC may increase by a factor of 10 as altitude increases from the surface to the lower stratosphere (Samset and Myhre, 2011), whereas forcing associated with the semi-direct effect (i.e. changes in cloudiness due to local heating from BC) becomes more negative as altitude increases (Samset and Myhre, 2015). On the other

Long-range transport of black carbon to the Pacific Ocean

J. Zhang et al.

Title Page

Abstract

Introduction

Conclusions

References

Tables

Figures



Back

Close

Full Screen / Esc

Printer-friendly Version

Interactive Discussion



Long-range transport of black carbon to the Pacific Ocean

J. Zhang et al.

Title Page

Abstract

Introduction

Conclusions

References

Tables

Figures



Back

Close

Full Screen / Esc

Printer-friendly Version

Interactive Discussion



uncertainty in predicting BC concentrations over remote regions (Textor et al., 2007; Schwarz et al., 2010). As emitted, BC is mostly hydrophobic (Laborde et al., 2013), but can become coated by water-soluble components through atmospheric aging processes. The coatings transits BC from being hydrophobic to hydrophilic, allowing the BC-containing particles to become cloud condensation nuclei and be scavenged by precipitation (Riemer et al., 2010; Oshima and Koike, 2013). Exponential timescale for this aging process to occur, the so-called “aging timescale”, therefore highly influences the timing of cloud formation and wet deposition, and thus is of great research interest (Liu et al., 2011). The thickness of BC coatings have been observed to increase with aging at the remote marine Pico Mountain Observatory, which shows that the fraction of coated particles for plumes with an age of ~ 15.7 days is 87 %, higher than that of ~ 9.5 days (57 %) (China et al., 2015). Quantitatively relating the age of BC-containing particles to its hygroscopicity using observations is very challenging (McMeeking et al., 2011). Laboratory measurements show that BC particles are considerably hygroscopic after being coated by condensed H_2SO_4 (Zhang et al., 2008), or when a sulfur-containing compound is added to the diesel fuel itself, presumably also leading to a sulfuric coating (Lammel and Novakov, 1995). The oxidation of organic coatings on BC by ozone and nitrogen oxide is also highlighted as an important pathway to aging in chamber studies (Kotzick et al., 1997; Kotzick and Niessner, 1999). Another study reporting observations in the United Kingdom finds that nitrate is the primary component of the coating on BC that leads to substantial increases in hygroscopicity (D. Liu et al., 2013). In principle, the conversion of hydrophobic to hydrophilic BC is very complicated, involving coagulation with sulfate and nitrate, condensation of nitric and sulfuric acid, and oxidation of organic coatings (Riemer et al., 2004; Matsui and Koike, 2012).

The aforementioned uncertainties in process and timescale for atmospheric aging, which converts BC from being hydrophobic to hydrophilic, leads to significant uncertainties in the transport of BC from source regions to remote areas. For example, previous studies that look at source regions of Arctic BC disagree on the relative importance of contributions from North American, Asian, and European emissions (Koch and

where v_d is dry deposition rate (m s^{-1}), r_a is aerodynamic resistance, r_s is surface_resistance, u^* is friction velocity (m s^{-1}), z_0 is the roughness length (m), z_i is boundary layer depth (m), and L is the Monin-Obukhov length (m). As a result, dry deposition velocity depends on surface properties (e.g. vegetation type).

For in-cloud wet scavenging of BC, we follow the parameterization used in Liu et al. (2011). The first-order in-cloud scavenging rate coefficient (s^{-1}) is expressed as

$$K_{\text{in}} = \frac{P_{\text{rain}}F_{\text{liq}} + P_{\text{snow}}F_{\text{ice}} + P_{\text{conv}}F_{\text{conv}}}{C} \quad (2)$$

where P_{rain} , P_{snow} , and P_{conv} are the rates of stratiform rain precipitation, stratiform snow precipitation, and convective precipitation ($\text{kg m}^{-3} \text{s}^{-1}$), respectively, and C is the cloud water content (kg m^{-3}). For convective clouds, F_{conv} is the fraction of in-cloud hydrophilic BC that is incorporated into cloud droplets or ice crystals. For stratiform clouds, F_{liq} (F_{ice}) is the fraction of in-cloud hydrophilic BC that is incorporated into liquid cloud droplets (ice crystals).

As previous studies indicate, the fraction of BC that is incorporated in cloud droplets or ice crystals decreases as temperature decreases and ice mass fraction increases in mixed-phase clouds (Croft et al., 2010, 2012; Liu et al., 2011; Fan et al., 2012). This phenomenon is attributable to the so-called Bergeron process, by which ice crystals grow rapidly at the expense of liquid droplets, leaving BC-containing cloud nuclei interstitial (i.e. not activated) (Cozic et al., 2007). However, the Bergeron process is not important in deep convective clouds where ice forms rapidly via rimming or accretion. Thus, generally $F_{\text{ice}} < F_{\text{liq}} < F_{\text{conv}}$. In this study, we set $F_{\text{ice}} = 0.1$, $F_{\text{liq}} = 0.5$, and $F_{\text{conv}} = 1.0$ as referenced to previous studies (Liu et al., 2011; Wang et al., 2011; Hodnebrog et al., 2014).

2.3 HIAPER Pole-to-Pole Observations

The HIPPO campaigns unprecedentedly provide vertical profiles from the surface to upper troposphere for 26 species over the Pacific Ocean, spanning from approximately

Long-range transport of black carbon to the Pacific Ocean

J. Zhang et al.

Title Page

Abstract

Introduction

Conclusions

References

Tables

Figures



Back

Close

Full Screen / Esc

Printer-friendly Version

Interactive Discussion



Long-range transport of black carbon to the Pacific Ocean

J. Zhang et al.

Title Page

Abstract

Introduction

Conclusions

References

Tables

Figures



Back

Close

Full Screen / Esc

Printer-friendly Version

Interactive Discussion



90° N to 70° S, in different seasons (Wofsy et al., 2011). BC is measured by a Single Particle Soot Photometer (SP2) using laser-induced incandescence (Schwarz et al., 2010). The SP2 heats BC-containing particles to its vaporization temperature and measures the resulting incandescence emitted by the BC core. Since the intensity of incandescence responds linearly to the mass of refractory BC, SP2 measures BC mass independent of particles morphology and mixing state (Schwarz et al., 2006; Schwarz et al., 2008). We constrain and evaluate our model by comparing simulated vertical profiles of BC mass mixing ratios over the central Pacific Ocean to observations from five field deployments (HIPPO I on 08 January–30 January 2009; HIPPO II on 31 October–22 November 2009; HIPPO III on 24 March–16 April 2010; HIPPO IV on 14 June–11 July 2011; HIPPO V on 09 August–09 September 2011). Note that we use only the HIPPO observations taken in the Central Pacific Ocean (130° W–160° E) and ignore observations near source regions.

2.4 Tracer tagging and sensitivity simulations

In this study, we add 13 tracers to the model to explicitly track BC emissions from non-overlapping geopolitical regions, an approach often called “tagging” (Rasch et al., 2000). Tagging is more accurate and less computationally consuming than the widely used emission sensitivity approach (Wang et al., 2014). We expand the ten defined continental regions in Liu et al. (2009) to thirteen source regions to better distinguish the differences in climate and emission source type between regions. As shown in Fig. 1, the tagged source regions are Canada (CA), North America except Canada (NA), East Asia (EA), the former Soviet Union (SU), Europe (EU), Africa (AF), South America (SA), the Indian subcontinent (IN), Australia (AU), Middle Asia (MA), Southeast Asia (SE), the Middle East (ME), and the rest regions (RR). For each simulation, the tagged tracers undergo transport and deposition processes in the same way as untagged BC. Since all the chemical and physical processes involving BC are nearly linear in MOZART-4, the sum of the 13 regional BC tracers is approximately equal to the untagged BC.

in their source types (e.g. anthropogenic, biomass burning) and concentrations of oxidants. Therefore, BC emitted from different regions should undergo aging with different timescales.

In this study, we optimize the aging timescales of BC emitted from thirteen source regions to best match the HIPPO observations. For each HIPPO deployment, we compare observations vs. simulations from 70° S to 90° N and 0 to 10 km along the HIPPO trajectory. The absolute deviation between modeled BC (BC_m) and observed BC (BC_o) mass mixing ratios for each latitude and altitude is calculated, and the average of normalized mean absolute error (NMAE) is then used as an indicator of the model performance in each deployment:

$$NMAE = \frac{1}{N} \sum_{nlat} \sum_{nalt} \frac{Abs(BC_m(j, k) - BC_o(j, k))}{Min(BC_m(j, k), BC_o(j, k))}, \quad (3)$$

where j indexes latitude bins, k indexes altitude bins, $nlat = 16$ is the total number of latitude bins (every 10° from 70° S to 90° N), and $nalt = 10$ is the total number of altitude bins (every 1 km from 0 to 10 km). $Abs(BC_m(j, k) - BC_o(j, k))$ represents the absolute value of modeled BC minus observed BC averaged over the j th and k th latitude and altitude bin. N is the total number of latitude and altitude bins with recorded HIPPO observations. We normalize the absolute errors by the minimum of observed and modeled BC so that NMAE weights both high bias and low bias equally. Unlike the root mean square error, the NMAE does not amplify the importance of the outliers.

Aging timescale affects atmospheric concentrations of BC through its influence on hygroscopicity and wet deposition of the particle. Thus, BC_m and NMAE are functions of aging timescale. Given the 13 simulations, each assuming a different aging timescale for BC (i.e. 4, 8, 12, 18, 24, 27.6, 38.4, 48, 60, 90, 120, 160, 200 h), and the 13 tagged tracers for BC emissions from each source region, we determine the best-fit aging timescale for each source region by minimizing NMAE. Note that we assume the aging rates of BC emitted from Africa, South America, and Australia to be the same since these three regions are all biomass burning dominated sources in the Southern Hemi-

Long-range transport of black carbon to the Pacific Ocean

J. Zhang et al.

[Title Page](#)[Abstract](#)[Introduction](#)[Conclusions](#)[References](#)[Tables](#)[Figures](#)[Back](#)[Close](#)[Full Screen / Esc](#)[Printer-friendly Version](#)[Interactive Discussion](#)

sphere, effectively reducing the total number of tagged tracers from 13 to 11. Thus, we determine best-fit BC aging timescale for each source region (out of 13^{11} combinations in total) that minimizes NMAE.

3 Optimized BC profiles over the Pacific Ocean

To give a sense of the influence of aging timescale on BC, global BC burdens for the minimum and maximum aging timescales considered here (i.e. 4 and 200 h) are shown in Fig. 2. BC burden increases with aging timescale in both the lower (Fig. 2d, e) and mid and upper troposphere (Fig. 2a, b). For most regions, BC burden in remote areas and in the mid and upper troposphere is more sensitive to aging timescale than that in source regions and in the lower troposphere (Fig. 2c, f). BC over the Pacific Ocean increases by a factor of 5–100 as the aging timescale increases from 4 to 200 h (Fig. 2c, f).

The dominant regional contributors to annual averaged BC burden for aging timescales of 4 and 200 h are shown in Fig. 3. Longer aging timescales increase the footprint areas dominated by the highest emitting source regions. For example, the area over the Pacific Ocean for which East Asian emissions dominate the burden is larger when aging timescale is 200 vs. 4 h. Over source regions, BC in the lower troposphere is dominated by local emissions for both aging timescales. However, the dominant source of BC in the mid and upper troposphere over source regions can switch from local source emissions to long-range transport from other source regions when increasing aging timescale. For example, BC in the mid and upper troposphere over the United States is dominated by local emissions when aging timescale is 4 h, but dominated by East Asian emissions when aging timescale is 200 h. Thus, varying aging timescale can lead to substantial differences in BC simulation over the Pacific Ocean, supporting the need to constrain the aging timescale by observations.

Optimized aging timescales for each source region and season are shown in Table 1. Values differ significantly by source region and season. We find that the aging of BC

Long-range transport of black carbon to the Pacific Ocean

J. Zhang et al.

Title Page

Abstract

Introduction

Conclusions

References

Tables

Figures



Back

Close

Full Screen / Esc

Printer-friendly Version

Interactive Discussion



both pattern and magnitude. NMAE is reduced significantly for each latitude band and HIPPO campaign, with reductions ranging from a factor of 2 to 25 (Fig. 4). Campaign-averaged NMAE is also reduced by a factor of 4–10 (Table 1). For comparison, we also derive the normalized mean bias used in Samset et al. (2014). Values for the improved model are below 25% for every campaign (Table 1), lower than their reported NMB for most AeroCom models. Figure S1 in the Supplement shows that the improved model also agrees with the surface air observations of BC in source regions over the United States, Europe and East Asia.

Differences between the improved model and observations remain in a few cases. Higher modeled vs. observed BC in the tropics and in the northern mid-latitudes during HIPPO5 is likely due to the misrepresentation of clouds and precipitation in MOZART-4. As shown in Figs. S1 and S2 (in the Supplement), precipitation predicted by MOZART-4 is generally less than NCEP reanalysis in the source regions of BC along the HIPPO5 trajectory (e.g. East Asia and Canada). Lower modeled vs. observed BC in the Southern Hemisphere during HIPPO5 could stem from the fact that the model uses a monthly biomass burning emission inventory. This means that emissions lack daily variation in biomass burning activities that could be important in reality where biomass burning emissions dominate BC loading. BC mass mixing ratios in the mid and upper troposphere over the South Pacific Ocean during HIPPO5 are higher than that during HIPPO1-4 by at least a factor of 2, implying that HIPPO5 might include abrupt emissions events that are not captured by the model.

4 Regional contribution of source regions to BC loading

Seasonally varying optimized aging timescales for each source region are used to investigate the dominant source regions contributing to zonal mean mass mixing ratio of BC over the Pacific Ocean (130° W–160° E) (Fig. 5a), and column burden of BC around the globe (Fig. 5b). We assume that optimized aging timescales for HIPPO1, 2, 3 and 4 are representative for DJF, SON, MAM, and JJA, respectively (see Table 1). BC in

Long-range transport of black carbon to the Pacific Ocean

J. Zhang et al.

Title Page

Abstract

Introduction

Conclusions

References

Tables

Figures



Back

Close

Full Screen / Esc

Printer-friendly Version

Interactive Discussion



Long-range transport of black carbon to the Pacific Ocean

J. Zhang et al.

Title Page

Abstract

Introduction

Conclusions

References

Tables

Figures



Back

Close

Full Screen / Esc

Printer-friendly Version

Interactive Discussion



the lower troposphere over the Pacific Ocean is mostly controlled by either emissions from RR (“rest regions”, i.e. ships), or the closest upwind source regions like Australia, South America and East Asia (Fig. 5a). On the other hand, BC in the mid and upper troposphere is influenced mostly by BC emissions from major source regions: East Asia, Australia, South America, Africa, and North America. East Asian BC emissions, which are mainly of anthropogenic origin, dominate BC loading over the Northern Pacific Ocean even though its aging is fast. Also, as shown in Fig. 5b, the Arctic BC is dominated by European emissions, while BC in the Antarctica is dominated by South American emissions.

The relative contribution of emissions from each source region to BC burden over each receptor region is presented in Table 2. We add an extra receptor region, the central Pacific Ocean (PO), defined as 60° S–58° N, 160° E–130° W. In PO, the dominant contributor is East Asia, accounting for 26 % of the burden. In the former Soviet Union, middle Asia, and Canada, local emissions account for no more than 50 % of the BC burden, whereas Europe contributes 44, 43, and 14 % to their burdens, respectively. BC over other regions is dominated by local sources. For example, local sources are responsible for 89, 77, and 73 % of the BC burden in India, East Asia and North America. Thus, controlling local anthropogenic sources is expected to have the largest impact on BC burdens in these regions.

Table 3 compares the annual mean (2009–2011 average) dry deposition flux, wet deposition flux, burden, and lifetime for BC emitted from different source regions. The lifetime of BC estimated by the improved model is 4.9 days. This lifetime is quite similar to that from recent studies (Wang et al., 2014, and Hodnebrog et al., 2014). They modify model scavenging processes to better reproduce HIPPO observations, and find that BC lifetimes are shortened from 5.9 to 4.2 days, and from 6.3 to 3.9 days, respectively. In addition, Samset et al. (2014) find that while the lifetime of BC is 6.8 ± 1.8 days averaged over 13 AeroCom models, the models with lifetime less than 5 days best match HIPPO observations. Our result is in accordance with their conclusions, and is lower than the BC lifetime of 6.1 days estimated by Bond et al. (2013).

Long-range transport of black carbon to the Pacific Ocean

J. Zhang et al.

Title Page

Abstract

Introduction

Conclusions

References

Tables

Figures



Back

Close

Full Screen / Esc

Printer-friendly Version

Interactive Discussion



Table 3 also shows that the lifetime of BC varies significantly by source region, ranging from 2 to 10 days. Regional variation in the lifetime of BC is likely caused by differences in wet scavenging, which depends on precipitation patterns and the hygroscopicity of BC-containing particles. The lifetimes of BC emitted from the former Soviet Union (4.4 days), East Asia (2.2 days), North America (3.7 days) and Southeast Asia (3.1 days) are shorter than the corresponding global average. Given the wide range of BC lifetime by source region, the relative contribution of different regions to burdens is not well characterized by the relative rates of emissions. For example, although East Asia emits the largest amount of BC, its lifetime is the shortest (~ 2 days). This means that the contribution of East Asian emissions to the global BC burden is only 1/3 of that of the second-leading source region (Africa). Using a different model and a rough division of source regions, Wang et al. (2014) also find that the lifetimes of East Asian (2.8 days), Southeast Asian (2.1 days), and American BC emissions (3.0 days) are shorter than the global average lifetime (4.7 days).

5 Dependence of BC lifetime on aging timescale

In this section, we further investigate the dependence of lifetime (derived by the annual mean burden and removal flux) on aging timescale for BC emitted from different source regions. As shown in Fig. 6, the lifetime of BC originating from different regions increases approximately linearly with aging timescale. Although there is variation in the y-intercepts for curves of lifetime vs. aging timescale, slopes are quite similar. In an effort to understand the drivers of the relationship between lifetime T (h) and aging timescale τ (h), we derive a theoretical description here. Taking the global atmosphere as a box, the mass balance for B_1 (annual mean hydrophobic BC burden, units of kg) and B_2 (annual mean hydrophilic BC burden, units of kg) are

$$\frac{dB_1}{dt} = (1 - \alpha)E - \frac{B_1}{\tau} - K_D B_1 \quad (4)$$

$$\frac{dB_2}{dt} = \alpha E + \frac{B_1}{\tau} - (K_D + K_W)B_2 \quad (5)$$

where α is the fraction of BC emitted that is hydrophilic, E (kg h^{-1}) is the annual mean emission rate, and K_D and K_W are the first-order dry and wet deposition coefficients (h^{-1}), respectively. K_W accounts for both precipitation intensity and scavenging efficiency.

Assuming that both hydrophilic and hydrophobic BC is in steady state, we derive the lifetime of BC as:

$$T = \frac{B_1 + B_2}{E} = \frac{((1 - \alpha)K_W + K_D)\tau + 1}{(1 + K_D\tau)(K_D + K_W)} \quad (6)$$

If further assuming that K_D and K_W are not dependent on τ , we then derive the slope (Eq. 7) and intercept (Eq. 8) of the $T - \tau$ curve:

$$\frac{dT}{d\tau} = \frac{(1 - \alpha)K_W}{(K_D + K_W)(1 + K_D\tau)^2} \quad (7)$$

$$T(\tau = 0) = \frac{1}{K_W + K_D} \quad (8)$$

The slope ($\frac{dT}{d\tau}$) represents the sensitivity of BC lifetime to aging timescale, which is a function of wet and dry deposition coefficients of BC, and the fraction of BC emitted that is hydrophilic. Given Equation 7, if $\alpha = 1$ then $\frac{dT}{d\tau} = 0$, implying that all BC is aged and therefore hydrophilic as emitted. If $K_D = 0$ then $\frac{dT}{d\tau} = 1 - \alpha$. Therefore, if K_D is negligible, the lifetime of BC will be linearly related to aging timescale. In addition, lower fractions of hydrophilic BC in emissions (α) will lead to larger sensitivities of BC lifetime to aging timescale ($\frac{dT}{d\tau}$). In MOZART-4, α is assumed to be 0.2 for all emission sources. So if K_D

Long-range transport of black carbon to the Pacific Ocean

J. Zhang et al.

Title Page	
Abstract	Introduction
Conclusions	References
Tables	Figures
◀	▶
◀	▶
Back	Close
Full Screen / Esc	
Printer-friendly Version	
Interactive Discussion	



is negligible, the theoretical slope of the $T - \tau$ curve is 0.8, which is very close to the curve for untagged BC (black line) in Fig. 6.

The intercepts of $T - \tau$ curves represent the lifetime of BC when the aging process is extremely fast (i.e. low values of aging timescale) such that all emitted BC can be regarded to be hydrophilic. As shown by Eq. (8), the intercept is a function of local wet deposition coefficient and dry deposition coefficient. Intercepts of the $T - \tau$ curves vary by source, ranging from 40 to 170 h. BC emitted in the Middle East, Africa, Canada, Australia, and South America has a larger intercept than the untagged BC because the climate in these regions lacks precipitation. The Middle East is dry and lacks precipitation in general, and emissions from Africa, Canada, and Australia are mainly from biomass burning activities that usually occur during their dry seasons.

It should be noted that in our derivation of Eqs. (7) and (8), we assume that K_D and K_W are independent of τ . In reality, however, K_D and K_W can depend on τ . For example, as aging timescale increases, BC has a longer lifetime and is more likely to encounter precipitation in regions farther away from the source. Nonetheless, the discussion above helps elucidate that the dependence of lifetime on aging timescale is determined by the fraction of emitted BC that is hydrophilic, and the factors that influence dry and wet deposition (e.g. precipitation).

Since the aging timescale varies by region and season, the common practice in modeling of setting a fixed global uniform aging rate may lead to significant misrepresentation of BC lifetime and burden. Employing realistic aging timescales is especially important for regions shown in Fig. 6 with the highest slopes and lowest intercepts; changes in aging timescale would lead to the largest relative changes in BC lifetime in these regions. For instance, for Southeast Asia, increasing the aging timescale of BC from 0 to 60 h nearly doubles its lifetime.

Policies that control SO_2 and other soluble compounds may slow BC aging, increase the lifetime of BC, and partially offset efforts made on BC mitigation. For example, as indicated by a chamber study, employing after-treatment technologies such as oxidation catalysts in combustion systems can reduce emissions of volatile organic compounds

Long-range transport of black carbon to the Pacific Ocean

J. Zhang et al.

[Title Page](#)[Abstract](#)[Introduction](#)[Conclusions](#)[References](#)[Tables](#)[Figures](#)[Back](#)[Close](#)[Full Screen / Esc](#)[Printer-friendly Version](#)[Interactive Discussion](#)

and formation of secondary organic aerosols (SOA) that could internally mix with BC, ultimately slowing the aging of BC (Tritscher et al., 2011). Thus, policies for protecting human health that target reductions in emissions of only fine soluble particulate matter (i.e., sulfate, nitrate and SOA) could increase BC burden through increases in aging timescale, and potentially enhances its positive radiative forcing.

6 Caveats

We note that there are limitations to our approach. First, we assume that model parameterizations of wet and dry deposition, transport, and emissions are realistic, even though these processes also affect BC distributions and include uncertainties (Vignati et al., 2010; Fan et al., 2012). Consequently, the optimized aging timescales may partially counter biases in these processes (i.e. other than aging), and may vary according to the model used. Also, only HIPPO is used in our study. For some source regions, observations in other remote regions would provide a better constraint for optimizing aging timescale in the model. More specifically, aircraft observations over the Atlantic Ocean could better constrain aging timescales for BC emitted from Africa and South America. As new observations become available, this study could be repeated to optimize the aging timescale for all source regions. BC aging includes complicated chemistry and physics, and is simplified in our modeling as a first-order conversion from hydrophobic to hydrophilic BC. Nevertheless, the goal of our aging optimization is not to provide an aging timescale that can be directly used in models (since models differ significantly in parameterizing wet scavenging efficiency), but to estimate the spatiotemporal pattern of aging timescales globally using every HIPPO observation.

7 Conclusions

In this study, we tag BC emitted from thirteen regions around the globe, and conduct a set of sensitivity simulations to investigate how different aging timescales affect spa-

Long-range transport of black carbon to the Pacific Ocean

J. Zhang et al.

Title Page

Abstract

Introduction

Conclusions

References

Tables

Figures



Back

Close

Full Screen / Esc

Printer-friendly Version

Interactive Discussion



Long-range transport of black carbon to the Pacific Ocean

J. Zhang et al.

Title Page

Abstract

Introduction

Conclusions

References

Tables

Figures



Back

Close

Full Screen / Esc

Printer-friendly Version

Interactive Discussion



tial distributions and source-receptor relationships for BC in a global chemical transport model, MOZART-4. We find that BC burden and source-receptor relationships are remarkably sensitive to the assumed aging timescale in the model; this motivates our use of HIPPO observations to optimize BC aging timescale by minimizing model-measurement differences. Physically-based dry and wet deposition schemes and optimized aging timescales for different regions are employed in MOZART-4, which significantly improves the model's performance over the Pacific Ocean relative to the default model; the campaign-averaged normalized mean absolute error is reduced by a factor of 4–10. The optimized aging timescales vary greatly by source region and season. In the Northern Hemisphere, we find that the aging timescale for BC emitted in mid- and low-latitude locations is in general less than half a day, whereas that for BC emitted from high-latitude locations in most seasons (i.e. Spring, Fall, and Winter) is 4–8 days.

Using the improved model, we find that the dominant contributors to BC in the lower troposphere over the central Pacific Ocean are local sources (i.e. ship emissions), Australia, South America and East Asia. For the mid and upper troposphere over the Pacific Ocean, the dominant sources are East Asia, Australia, South America, Africa, and North America. East Asian emissions contribute the most (26 %) to the total burden of tropospheric BC over the Pacific Ocean. We also find that BC emitted from different source regions has distinct atmospheric lifetimes, suggesting that comparing only emissions of different regions does not directly predict their contribution to burden and therefore climate consequences. The lifetimes of BC emitted from East Asia, Southeast Asia, North America, and the former Soviet Union are 2.2, 3.2, 3.8, and 4.4 days respectively, shorter than 4.9 days, the global average lifetime.

Using model sensitivity simulations we determine the sensitivity of BC lifetime to aging timescale for emissions from each source region. The lifetime-aging timescale relationship is for most regions nearly linear. The sensitivity is influenced by wet and dry deposition rates, and more importantly by a parameter that describes the fraction of BC emissions that are emitted directly as hydrophilic.

Long-range transport of black carbon to the Pacific Ocean

J. Zhang et al.

Title Page

Abstract

Introduction

Conclusions

References

Tables

Figures



Back

Close

Full Screen / Esc

Printer-friendly Version

Interactive Discussion



Future observations that speciate coatings on BC and measure hygroscopicity of both freshly emitted and aged BC in different regions and seasons are needed to further constrain aging timescales and understand the physics and chemistry of the aging process. The lifetime of BC determines its global reach, and consequently its radiative forcing on the climate system. BC with slow aging timescales and long lifetimes can influence the climate in remote areas substantially (e.g. over the oceans and the Arctic). In principle, the estimated climate impacts of BC emitted from different regions rely on the representation of particles' hygroscopicity and the assumptions on aging timescales. Our study highlights the importance of accurately representing aging processes in models and parameterizing aging timescales differently in different regions and seasons.

We recommend that future inter-model comparisons like AeroCom use tagging techniques to compare model estimates of the lifetimes of BC emitted from different regions. The tracer tagging technique utilized here can also be used to estimate regional source contributions to BC observed in future aircraft campaigns, to help choose locations for future campaigns, and to attribute discrepancies in inter-model comparisons to specific source regions.

The Supplement related to this article is available online at doi:10.5194/acpd-15-16945-2015-supplement.

Acknowledgements. We thank Xiaoyuan Li, Cenlin He, Wei Tao, Jing Meng, Huizhong Shen, Maowei Wu, Zhaoyi Shen, Kan Chen and Yan Xia for their helpful contributions and suggestions to this study. This work was supported by funding from the National Natural Science Foundation of China under awards 41222011, 41390241 and 41130754, the Research Project of the Chinese Ministry of Education No. 113001A, the undergraduate student research training program, and the 111 Project (B14001).

References

- Ban-Weiss, G. A., Cao, L., Bala, G., and Caldeira, K.: Dependence of climate forcing and response on the altitude of black carbon aerosols, *Clim. Dynam.*, 38, 897–911, doi:10.1007/s00382-011-1052-y, 2012.
- 5 Bell, M. L., Ebisu, K., Peng, R. D., Samet, J. M., and Dominici, F.: Hospital Admissions and Chemical Composition of Fine Particle Air Pollution, *Am. J. Resp. Crit. Care.*, 179, 1115–1120, doi:10.1164/rccm.200808-1240OC, 2009.
- Bian, H., Colarco, P. R., Chin, M., Chen, G., Rodriguez, J. M., Liang, Q., Blake, D., Chu, D. A., da Silva, A., Darmenov, A. S., Diskin, G., Fuelberg, H. E., Huey, G., Kondo, Y., Nielsen, J. E.,
10 Pan, X., and Wisthaler, A.: Source attributions of pollution to the Western Arctic during the NASA ARCTAS field campaign, *Atmos. Chem. Phys.*, 13, 4707–4721, doi:10.5194/acp-13-4707-2013, 2013.
- Bollasina, M. A., Ming, Y., and Ramaswamy, V.: Anthropogenic Aerosols and the Weakening of the South Asian Summer Monsoon, *Science*, 334, 502–505, doi:10.1126/science.1204994, 2011.
15
- Bollasina, M. A., Ming, Y., Ramaswamy, V., Schwarzkopf, M. D., and Naik, V.: Contribution of local and remote anthropogenic aerosols to the twentieth century weakening of the South Asian Monsoon, *Geophys. Res. Lett.*, 41, 680–687, doi:10.1002/2013gl058183, 2014.
- Bond, T. C., Doherty, S. J., Fahey, D. W., Forster, P. M., Berntsen, T., DeAngelo, B. J., Flanner, M. G., Ghan, S., Karcher, B., Koch, D., Kinne, S., Kondo, Y., Quinn, P. K., Sarofim, M. C., Schultz, M. G., Schulz, M., Venkataraman, C., Zhang, H., Zhang, S., Bellouin, N., Guttikunda, S. K., Hopke, P. K., Jacobson, M. Z., Kaiser, J. W., Klimont, Z., Lohmann, U., Schwarz, J. P., Shindell, D., Storelvmo, T., Warren, S. G., and Zender, C. S.: Bounding the role of black carbon in the climate system: A scientific assessment, *J. Geophys. Res.-Atmos.*, 118, 5380–5552, doi:10.1002/Jgrd.50171, 2013.
20
- Bourgeois, Q. and Bey, I.: Pollution transport efficiency toward the Arctic: Sensitivity to aerosol scavenging and source regions, *J. Geophys. Res.*, 116, D08213, doi:10.1029/2010jd015096, 2011.
- Cheng, Y. F., Su, H., Rose, D., Gunthe, S. S., Berghof, M., Wehner, B., Achtert, P., Nowak, A., Takegawa, N., Kondo, Y., Shiraiwa, M., Gong, Y. G., Shao, M., Hu, M., Zhu, T., Zhang, Y. H., Carmichael, G. R., Wiedensohler, A., Andreae, M. O., and Pöschl, U.: Size-resolved measurement of the mixing state of soot in the megacity Beijing, China: diurnal cycle, aging
25
- 30

Long-range transport of black carbon to the Pacific Ocean

J. Zhang et al.

Title Page

Abstract

Introduction

Conclusions

References

Tables

Figures



Back

Close

Full Screen / Esc

Printer-friendly Version

Interactive Discussion



**Long-range transport
of black carbon to the
Pacific Ocean**

J. Zhang et al.

[Title Page](#)[Abstract](#)[Introduction](#)[Conclusions](#)[References](#)[Tables](#)[Figures](#)[Back](#)[Close](#)[Full Screen / Esc](#)[Printer-friendly Version](#)[Interactive Discussion](#)

and parameterization, *Atmos. Chem. Phys.*, 12, 4477–4491, doi:10.5194/acp-12-4477-2012, 2012.

China, S., Scarnato, B., Owen, R. C., Zhang, B., Ampadu, M. T., Kumar, S., Dzepina, K., Dziobak, M. P., Fialho, P., Perlinger, J. A., Hueber, J., Helmig, D., Mazzoleni, L. R., and Mazzoleni, C.: Morphology and mixing state of aged soot particles at a remote marine free troposphere site: Implications for optical properties, *Geophys. Res. Lett.*, 42, 1243–1250, doi:10.1002/2014gl062404, 2015.

Cozic, J., Verheggen, B., Mertes, S., Connolly, P., Bower, K., Petzold, A., Baltensperger, U., and Weingartner, E.: Scavenging of black carbon in mixed phase clouds at the high alpine site Jungfraujoch, *Atmos. Chem. Phys.*, 7, 1797–1807, doi:10.5194/acp-7-1797-2007, 2007.

Croft, B., Lohmann, U., Martin, R. V., Stier, P., Wurzler, S., Feichter, J., Hoose, C., Heikkilä, U., van Donkelaar, A., and Ferrachat, S.: Influences of in-cloud aerosol scavenging parameterizations on aerosol concentrations and wet deposition in ECHAM5-HAM, *Atmos. Chem. Phys.*, 10, 1511–1543, doi:10.5194/acp-10-1511-2010, 2010.

Croft, B., Pierce, J. R., Martin, R. V., Hoose, C., and Lohmann, U.: Uncertainty associated with convective wet removal of entrained aerosols in a global climate model, *Atmos. Chem. Phys.*, 12, 10725–10748, doi:10.5194/acp-12-10725-2012, 2012.

Emmons, L. K., Walters, S., Hess, P. G., Lamarque, J.-F., Pfister, G. G., Fillmore, D., Granier, C., Guenther, A., Kinnison, D., Laepple, T., Orlando, J., Tie, X., Tyndall, G., Wiedinmyer, C., Baughcum, S. L., and Kloster, S.: Description and evaluation of the Model for Ozone and Related chemical Tracers, version 4 (MOZART-4), *Geosci. Model Dev.*, 3, 43–67, doi:10.5194/gmd-3-43-2010, 2010.

Evan, A. T., Kossin, J. P., Chung, C., and Ramanathan, V.: Arabian Sea tropical cyclones intensified by emissions of black carbon and other aerosols, *Nature*, 479, 94–119, doi:10.1038/Nature10552, 2011.

Fan, S. M., Schwarz, J. P., Liu, J., Fahey, D. W., Ginoux, P., Horowitz, L. W., Levy, H., Ming, Y., and Spackman, J. R.: Inferring ice formation processes from global-scale black carbon profiles observed in the remote atmosphere and model simulations, *J. Geophys. Res.-Atmos.*, 117, D23205, doi:10.1029/2012jd018126, 2012.

Feng, H.: A 3-mode parameterization of below-cloud scavenging of aerosols for use in atmospheric dispersion models, *Atmos. Environ.*, 41, 6808–6822, doi:10.1016/j.atmosenv.2007.04.046, 2007.

Long-range transport of black carbon to the Pacific Ocean

J. Zhang et al.

Title Page

Abstract

Introduction

Conclusions

References

Tables

Figures



Back

Close

Full Screen / Esc

Printer-friendly Version

Interactive Discussion



Flanner, M. G., Zender, C. S., Randerson, J. T., and Rasch, P. J.: Present-day climate forcing and response from black carbon in snow, *J. Geophys. Res.-Atmos.*, 112, D11202, doi:10.1029/2006jd008003, 2007.

Gallagher, M. W., Nemitz, E., Dorsey, J. R., Fowler, D., Sutton, M. A., Flynn, M., and Duyzer, J.: Measurements and parameterizations of small aerosol deposition velocities to grassland, arable crops, and forest: Influence of surface roughness length on deposition, *J. Geophys. Res.-Atmos.*, 107, 4154, doi:10.1029/2001jd000817, 2002.

Granier, C., Bessagnet, B., Bond, T., D'Angiola, A., van der Gon, H. D., Frost, G. J., Heil, A., Kaiser, J. W., Kinne, S., Klimont, Z., Kloster, S., Lamarque, J. F., Liousse, C., Masui, T., Meleux, F., Mieville, A., Ohara, T., Raut, J. C., Riahi, K., Schultz, M. G., Smith, S. J., Thompson, A., van Aardenne, J., van der Werf, G. R., and van Vuuren, D. P.: Evolution of anthropogenic and biomass burning emissions of air pollutants at global and regional scales during the 1980–2010 period, *Clim. Change*, 109, 163–190, doi:10.1007/s10584-011-0154-1, 2011.

Hack, J. J.: Parameterization of moist convection in the National Center for Atmospheric Research community climate model (CCM2), *J. Geophys. Res.-Atmos.*, 99, 5551–5568, doi:10.1029/93jd03478, 1994.

Hansen, J. and Nazarenko, L.: Soot climate forcing via snow and ice albedos, *P. Natl. Acad. Sci. USA*, 101, 423–428, doi:10.1073/pnas.2237157100, 2004.

He, C. L., Li, Q. B., Liou, K. N., Takano, Y., Gu, Y., Qi, L., Mao, Y. H., and Leung, L. R.: Black carbon radiative forcing over the Tibetan Plateau, *Geophys. Res. Lett.*, 41, 7806–7813, doi:10.1002/2014gl062191, 2014.

Hodnebrog, O., Myhre, G., and Samset, B. H.: How shorter black carbon lifetime alters its climate effect, *Nat. Commun.*, 5, 5065, doi:10.1038/Ncomms6065, 2014.

Holtstlag, A. A. M. and Boville, B. A.: Local Versus Nonlocal Boundary-Layer Diffusion in a Global Climate Model, *J. Climate*, 6, 1825–1842, doi:10.1175/1520-0442(1993)006<1825:Lvnld>2.0.Co;2, 1993.

Horowitz, L. W., Walters, S., Mauzerall, D. L., Emmons, L. K., Rasch, P. J., Granier, C., Tie, X. X., Lamarque, J. F., Schultz, M. G., Tyndall, G. S., Orlando, J. J., and Brasseur, G. P.: A global simulation of tropospheric ozone and related tracers: Description and evaluation of MOZART, version 2, *J. Geophys. Res.-Atmos.*, 108, 4784, doi:10.1029/2002jd002853, 2003.

**Long-range transport
of black carbon to the
Pacific Ocean**

J. Zhang et al.

[Title Page](#)[Abstract](#)[Introduction](#)[Conclusions](#)[References](#)[Tables](#)[Figures](#)[Back](#)[Close](#)[Full Screen / Esc](#)[Printer-friendly Version](#)[Interactive Discussion](#)

Huang, Y., Wu, S., Dubey, M. K., and French, N. H. F.: Impact of aging mechanism on model simulated carbonaceous aerosols, *Atmos. Chem. Phys.*, 13, 6329–6343, doi:10.5194/acp-13-6329-2013, 2013.

Janssen, N. A. H., Hoek, G., Simic-Lawson, M., Fischer, P., van Bree, L., ten Brink, H., Keuken, M., Atkinson, R. W., Anderson, H. R., Brunekreef, B., and Cassee, F. R.: Black Carbon as an Additional Indicator of the Adverse Health Effects of Airborne Particles Compared with PM₁₀ and PM_{2.5}, *Environ. Health Persp.*, 119, 1691–1699, doi:10.1289/Ehp.1003369, 2011.

Johnson, K. S., Zuberi, B., Molina, L. T., Molina, M. J., Iedema, M. J., Cowin, J. P., Gaspar, D. J., Wang, C., and Laskin, A.: Processing of soot in an urban environment: case study from the Mexico City Metropolitan Area, *Atmos. Chem. Phys.*, 5, 3033–3043, doi:10.5194/acp-5-3033-2005, 2005.

Kaneyasu, N. and Murayama, S.: High concentrations of black carbon over middle latitudes in the North Pacific Ocean, *J. Geophys. Res.-Atmos.*, 105, 19881–19890, 2000.

Kipling, Z., Stier, P., Schwarz, J. P., Perring, A. E., Spackman, J. R., Mann, G. W., Johnson, C. E., and Telford, P. J.: Constraints on aerosol processes in climate models from vertically-resolved aircraft observations of black carbon, *Atmos. Chem. Phys.*, 13, 5969–5986, doi:10.5194/acp-13-5969-2013, 2013.

Koch, D. and Del Genio, A. D.: Black carbon semi-direct effects on cloud cover: review and synthesis, *Atmos. Chem. Phys.*, 10, 7685–7696, doi:10.5194/acp-10-7685-2010, 2010.

Koch, D. and Hansen, J.: Distant origins of Arctic black carbon: A Goddard Institute for Space Studies ModelE experiment, *J. Geophys. Res.-Atmos.*, 110, D04204, doi:10.1029/2004jd005296, 2005.

Koch, D., Schulz, M., Kinne, S., McNaughton, C., Spackman, J. R., Balkanski, Y., Bauer, S., Berntsen, T., Bond, T. C., Boucher, O., Chin, M., Clarke, A., De Luca, N., Dentener, F., Diehl, T., Dubovik, O., Easter, R., Fahey, D. W., Feichter, J., Fillmore, D., Freitag, S., Ghan, S., Ginoux, P., Gong, S., Horowitz, L., Iversen, T., Kirkevåg, A., Klimont, Z., Kondo, Y., Krol, M., Liu, X., Miller, R., Montanaro, V., Moteki, N., Myhre, G., Penner, J. E., Perlwitz, J., Pitari, G., Reddy, S., Sahu, L., Sakamoto, H., Schuster, G., Schwarz, J. P., Seland, Ø., Stier, P., Takegawa, N., Takemura, T., Textor, C., van Aardenne, J. A., and Zhao, Y.: Evaluation of black carbon estimations in global aerosol models, *Atmos. Chem. Phys.*, 9, 9001–9026, doi:10.5194/acp-9-9001-2009, 2009.

Long-range transport of black carbon to the Pacific Ocean

J. Zhang et al.

Title Page

Abstract

Introduction

Conclusions

References

Tables

Figures



Back

Close

Full Screen / Esc

Printer-friendly Version

Interactive Discussion



- Kotzick, R. and Niessner, R.: The effects of aging processes on critical supersaturation ratios of ultrafine carbon aerosols, *Atmos. Environ.*, 33, 2669–2677, doi:10.1016/S1352-2310(98)00315-X, 1999.
- Kotzick, R., Panne, U., and Niessner, R.: Changes in condensation properties of ultrafine carbon particles subjected to oxidation by ozone, *J. Aerosol. Sci.*, 28, 725–735, doi:10.1016/S0021-8502(96)00471-5, 1997.
- Laborde, M., Crippa, M., Tritscher, T., Jurányi, Z., Decarlo, P. F., Temime-Roussel, B., Marchand, N., Eckhardt, S., Stohl, A., Baltensperger, U., Prévôt, A. S. H., Weingartner, E., and Gysel, M.: Black carbon physical properties and mixing state in the European megacity Paris, *Atmos. Chem. Phys.*, 13, 5831–5856, doi:10.5194/acp-13-5831-2013, 2013.
- Lammel, G. and Novakov, T.: Water Nucleation Properties of Carbon-Black and Diesel Soot Particles, *Atmos. Environ.*, 29, 813–823, doi:10.1016/1352-2310(94)00308-8, 1995.
- Lau, N. C. and Nath, M. J.: A Model Study of the Air-Sea Interaction Associated with the Climatological Aspects and Interannual Variability of the South Asian Summer Monsoon Development, *J. Climate*, 25, 839–857, doi:10.1175/Jcli-D-11-00035.1, 2012.
- Li, J., Posfai, M., Hobbs, P. V., and Buseck, P. R.: Individual aerosol particles from biomass burning in southern Africa: 2, Compositions and aging of inorganic particles, *J. Geophys. Res.-Atmos.*, 108, 8484, doi:10.1029/2002jd002310, 2003.
- Lin, S. J. and Rood, R. B.: Multidimensional flux-form semi-Lagrangian transport schemes, *Mon. Weather Rev.*, 124, 2046–2070, doi:10.1175/1520-0493(1996)124<2046:Mffslt>2.0.Co;2, 1996.
- Liu, D., Allan, J., Whitehead, J., Young, D., Flynn, M., Coe, H., McFiggans, G., Fleming, Z. L., and Bandy, B.: Ambient black carbon particle hygroscopic properties controlled by mixing state and composition, *Atmos. Chem. Phys.*, 13, 2015–2029, doi:10.5194/acp-13-2015-2013, 2013.
- Liu, J. F., Fan, S. M., Horowitz, L. W., and Levy, H.: Evaluation of factors controlling long-range transport of black carbon to the Arctic, *J. Geophys. Res.-Atmos.*, 116, D04307, doi:10.1029/2010jd015145, 2011.
- Liu, Y. K., Liu, J. F., and Tao, S.: Interannual variability of summertime aerosol optical depth over East Asia during 2000–2011: a potential influence from El Nino Southern Oscillation, *Environ. Res. Lett.*, 8, 044034, doi:10.1088/1748-9326/8/4/044034, 2013.
- Ma, P.-L., Gattiker, J. R., Liu, X., and Rasch, P. J.: A novel approach for determining source-receptor relationships in model simulations: a case study of black carbon transport in north-

ern hemisphere winter, *Environ. Res. Lett.*, 8, 024042, doi:10.1088/1748-9326/8/2/024042, 2013.

Matsui, H. and Koike, M.: New source and process apportionment method using a three-dimensional chemical transport model: Process, Age, and Source region Chasing ALgorithm (PASCAL), *Atmos. Environ.*, 55, 399–409, doi:10.1016/j.atmosenv.2012.02.080, 2012.

McMeeking, G. R., Good, N., Petters, M. D., McFiggans, G., and Coe, H.: Influences on the fraction of hydrophobic and hydrophilic black carbon in the atmosphere, *Atmos. Chem. Phys.*, 11, 5099–5112, doi:10.5194/acp-11-5099-2011, 2011.

Ming, Y., Ramaswamy, V., and Persad, G.: Two opposing effects of absorbing aerosols on global-mean precipitation, *Geophys. Res. Lett.*, 37, L13701, doi:10.1029/2010gl042895, 2010.

Moteki, N., Kondo, Y., Miyazaki, Y., Takegawa, N., Komazaki, Y., Kurata, G., Shirai, T., Blake, D. R., Miyakawa, T., and Koike, M.: Evolution of mixing state of black carbon particles: Aircraft measurements over the western Pacific in March 2004, *Geophys. Res. Lett.*, 34, L11803, doi:10.1029/2006gl028943, 2007.

Oshima, N. and Koike, M.: Development of a parameterization of black carbon aging for use in general circulation models, *Geosci. Model Dev.*, 6, 263–282, doi:10.5194/gmd-6-263-2013, 2013.

Posfai, M., Simonics, R., Li, J., Hobbs, P. V., and Buseck, P. R.: Individual aerosol particles from biomass burning in southern Africa: 1. Compositions and size distributions of carbonaceous particles, *J. Geophys. Res.-Atmos.*, 108, 8483, doi:10.1029/2002jd002291, 2003.

Ramanathan, V. and Carmichael, G.: Global and regional climate changes due to black carbon, *Nat. Geosci.*, 1, 221–227, doi:10.1038/ngeo156, 2008.

Rasch, P. J., Barth, M. C., Kiehl, J. T., Schwartz, S. E., and Benkovitz, C. M.: A description of the global sulfur cycle and its controlling processes in the National Center for Atmospheric Research Community Climate Model, Version 3, *J. Geophys. Res.-Atmos.*, 105, 1367–1385, doi:10.1029/1999jd900777, 2000.

Riener, N., Vogel, H., and Vogel, B.: Soot aging time scales in polluted regions during day and night, *Atmos. Chem. Phys.*, 4, 1885–1893, doi:10.5194/acp-4-1885-2004, 2004.

Riener, N., West, M., Zaveri, R., and Easter, R.: Estimating black carbon aging time-scales with a particle-resolved aerosol model, *J. Aerosol. Sci.*, 41, 143–158, doi:10.1016/j.jaerosci.2009.08.009, 2010.

Long-range transport of black carbon to the Pacific Ocean

J. Zhang et al.

Title Page

Abstract

Introduction

Conclusions

References

Tables

Figures



Back

Close

Full Screen / Esc

Printer-friendly Version

Interactive Discussion



**Long-range transport
of black carbon to the
Pacific Ocean**

J. Zhang et al.

Title Page

Abstract

Introduction

Conclusions

References

Tables

Figures



Back

Close

Full Screen / Esc

Printer-friendly Version

Interactive Discussion



Samset, B. H. and Myhre, G.: Vertical dependence of black carbon, sulphate and biomass burning aerosol radiative forcing, *Geophys. Res. Lett.*, 38, L24802, doi:10.1029/2011gl049697, 2011.

Samset, B. H. and Myhre, G.: Climate response to externally mixed black carbon as a function of altitude, *J. Geophys. Res.-Atmos.*, 120, 2913–2927, doi:10.1002/2014jd022849, 2015.

Samset, B. H., Myhre, G., Schulz, M., Balkanski, Y., Bauer, S., Berntsen, T. K., Bian, H., Bellouin, N., Diehl, T., Easter, R. C., Ghan, S. J., Iversen, T., Kinne, S., Kirkevåg, A., Lamarque, J.-F., Lin, G., Liu, X., Penner, J. E., Seland, Ø., Skeie, R. B., Stier, P., Takemura, T., Tsigaridis, K., and Zhang, K.: Black carbon vertical profiles strongly affect its radiative forcing uncertainty, *Atmos. Chem. Phys.*, 13, 2423–2434, doi:10.5194/acp-13-2423-2013, 2013.

Samset, B. H., Myhre, G., Herber, A., Kondo, Y., Li, S.-M., Moteki, N., Koike, M., Oshima, N., Schwarz, J. P., Balkanski, Y., Bauer, S. E., Bellouin, N., Berntsen, T. K., Bian, H., Chin, M., Diehl, T., Easter, R. C., Ghan, S. J., Iversen, T., Kirkevåg, A., Lamarque, J.-F., Lin, G., Liu, X., Penner, J. E., Schulz, M., Seland, Ø., Skeie, R. B., Stier, P., Takemura, T., Tsigaridis, K., and Zhang, K.: Modelled black carbon radiative forcing and atmospheric lifetime in AeroCom Phase II constrained by aircraft observations, *Atmos. Chem. Phys.*, 14, 12465–12477, doi:10.5194/acp-14-12465-2014, 2014.

Satheesh, S. K.: *Letter to the Editor* Aerosol radiative forcing over land: effect of surface and cloud reflection, *Ann. Geophys.*, 20, 2105–2109, doi:10.5194/angeo-20-2105-2002, 2002.

Schwarz, J. P., Gao, R. S., Fahey, D. W., Thomson, D. S., Watts, L. A., Wilson, J. C., Reeves, J. M., Darbeheshti, M., Baumgardner, D. G., Kok, G. L., Chung, S. H., Schulz, M., Hendricks, J., Lauer, A., Karcher, B., Slowik, J. G., Rosenlof, K. H., Thompson, T. L., Langford, A. O., Loewenstein, M., and Aikin, K. C.: Single-particle measurements of midlatitude black carbon and light-scattering aerosols from the boundary layer to the lower stratosphere, *J. Geophys. Res.-Atmos.*, 111, D16207, doi:10.1029/2006jd007076, 2006.

Schwarz, J. P., Spackman, J. R., Fahey, D. W., Gao, R. S., Lohmann, U., Stier, P., Watts, L. A., Thomson, D. S., Lack, D. A., Pfister, L., Mahoney, M. J., Baumgardner, D., Wilson, J. C., and Reeves, J. M.: Coatings and their enhancement of black carbon light absorption in the tropical atmosphere, *J. Geophys. Res.-Atmos.*, 113, D03203, doi:10.1029/2007jd009042, 2008.

Schwarz, J. P., Spackman, J. R., Gao, R. S., Watts, L. A., Stier, P., Schulz, M., Davis, S. M., Wofsy, S. C., and Fahey, D. W.: Global-scale black carbon profiles observed in the remote atmosphere and compared to models, *Geophys. Res. Lett.*, 37, L18812, doi:10.1029/2010gl044372, 2010.

**Long-range transport
of black carbon to the
Pacific Ocean**

J. Zhang et al.

[Title Page](#)[Abstract](#)[Introduction](#)[Conclusions](#)[References](#)[Tables](#)[Figures](#)[Back](#)[Close](#)[Full Screen / Esc](#)[Printer-friendly Version](#)[Interactive Discussion](#)

Schwarz, J. P., Samset, B. H., Perring, A. E., Spackman, J. R., Gao, R. S., Stier, P., Schulz, M., Moore, F. L., Ray, E. A., and Fahey, D. W.: Global-scale seasonally resolved black carbon vertical profiles over the Pacific, *Geophys. Res. Lett.*, 40, 5542–5547, doi:10.1002/2013gl057775, 2013.

5 Shen, Z., Liu, J., Horowitz, L. W., Henze, D. K., Fan, S., H., Levy II, Mauzerall, D. L., Lin, J.-T., and Tao, S.: Analysis of transpacific transport of black carbon during HIPPO-3: implications for black carbon aging, *Atmos. Chem. Phys.*, 14, 6315–6327, doi:10.5194/acp-14-6315-2014, 2014.

10 Shindell, D. T., Chin, M., Dentener, F., Doherty, R. M., Faluvegi, G., Fiore, A. M., Hess, P., Koch, D. M., MacKenzie, I. A., Sanderson, M. G., Schultz, M. G., Schulz, M., Stevenson, D. S., Teich, H., Textor, C., Wild, O., Bergmann, D. J., Bey, I., Bian, H., Cuvelier, C., Duncan, B. N., Folberth, G., Horowitz, L. W., Jonson, J., Kaminski, J. W., Marmer, E., Park, R., Pringle, K. J., Schroeder, S., Szopa, S., Takemura, T., Zeng, G., Keating, T. J., and Zuber, A.: A multi-model assessment of pollution transport to the Arctic, *Atmos. Chem. Phys.*, 8, 5353–5372, doi:10.5194/acp-8-5353-2008, 2008.

15 Textor, C., Schulz, M., Guibert, S., Kinne, S., Balkanski, Y., Bauer, S., Bernsten, T., Berglen, T., Boucher, O., Chin, M., Dentener, F., Diehl, T., Feichter, J., Fillmore, D., Ginoux, P., Gong, S., Grini, A., Hendricks, J., Horowitz, L., Huang, P., Isaksen, I. S. A., Iversen, T., Kloster, S., Koch, D., Kirkevåg, A., Kristjansson, J. E., Krol, M., Lauer, A., Lamarque, J. F., Liu, X., Montanaro, V., Myhre, G., Penner, J. E., Pitari, G., Reddy, M. S., Seland, Ø., Stier, P., Takemura, T., and Tie, X.: The effect of harmonized emissions on aerosol properties in global models –an AeroCom experiment, *Atmos. Chem. Phys.*, 7, 4489–4501, doi:10.5194/acp-7-4489-2007, 2007.

20 Tritscher, T., Juranyi, Z., Martin, M., Chirico, R., Gysel, M., Heringa, M. F., DeCarlo, P. F., Sierau, B., Prevot, A. S. H., Weingartner, E., and Baltensperger, U.: Changes of hygroscopicity and morphology during ageing of diesel soot, *Environ. Res. Lett.*, 6, 034026, doi:10.1088/1748-9326/6/3/034026, 2011.

25 van der Werf, G. R., Randerson, J. T., Giglio, L., Collatz, G. J., Mu, M., Kasibhatla, P. S., Morton, D. C., DeFries, R. S., Jin, Y., and van Leeuwen, T. T.: Global fire emissions and the contribution of deforestation, savanna, forest, agricultural, and peat fires (1997–2009), *Atmos. Chem. Phys.*, 10, 11707–11735, doi:10.5194/acp-10-11707-2010, 2010.

**Long-range transport
of black carbon to the
Pacific Ocean**

J. Zhang et al.

[Title Page](#)[Abstract](#)[Introduction](#)[Conclusions](#)[References](#)[Tables](#)[Figures](#)[Back](#)[Close](#)[Full Screen / Esc](#)[Printer-friendly Version](#)[Interactive Discussion](#)

Vignati, E., Karl, M., Krol, M., Wilson, J., Stier, P., and Cavalli, F.: Sources of uncertainties in modelling black carbon at the global scale, *Atmos. Chem. Phys.*, 10, 2595–2611, doi:10.5194/acp-10-2595-2010, 2010.

Wang, H. L., Rasch, P. J., Easter, R. C., Singh, B., Zhang, R. D., Ma, P. L., Qian, Y., Ghan, S. J., and Beagley, N.: Using an explicit emission tagging method in global modeling of source-receptor relationships for black carbon in the Arctic: Variations, sources, and transport pathways, *J. Geophys. Res.-Atmos.*, 119, 12888–12909, doi:10.1002/2014jd022297, 2014.

Wang, Q., Jacob, D. J., Fisher, J. A., Mao, J., Leibensperger, E. M., Carouge, C. C., Le Sager, P., Kondo, Y., Jimenez, J. L., Cubison, M. J., and Doherty, S. J.: Sources of carbonaceous aerosols and deposited black carbon in the Arctic in winter-spring: implications for radiative forcing, *Atmos. Chem. Phys.*, 11, 12453–12473, doi:10.5194/acp-11-12453-2011, 2011.

Wofsy, S. C., Team, H. S., Team, C. M., and Team, S.: HIAPER Pole-to-Pole Observations (HIPPO): fine-grained, global-scale measurements of climatically important atmospheric gases and aerosols, *Philos. T. R. Soc. A*, 369, 2073–2086, doi:10.1098/rsta.2010.0313, 2011.

Zarzycki, C. M. and Bond, T. C.: How much can the vertical distribution of black carbon affect its global direct radiative forcing?, *Geophys. Res. Lett.*, 37, L20807, doi:10.1029/2010gl044555, 2010.

Zhang, G. J. and Mcfarlane, N. A.: Sensitivity of Climate Simulations to the Parameterization of Cumulus Convection in the Canadian Climate Center General-Circulation Model, *Atmos. Ocean.*, 33, 407–446, 1995.

Zhang, R. Y., Khalizov, A. F., Pagels, J., Zhang, D., Xue, H. X., and McMurry, P. H.: Variability in morphology, hygroscopicity, and optical properties of soot aerosols during atmospheric processing, *P. Natl. Acad. Sci. USA*, 105, 10291–10296, doi:10.1073/pnas.0804860105, 2008.

Long-range transport of black carbon to the Pacific Ocean

J. Zhang et al.

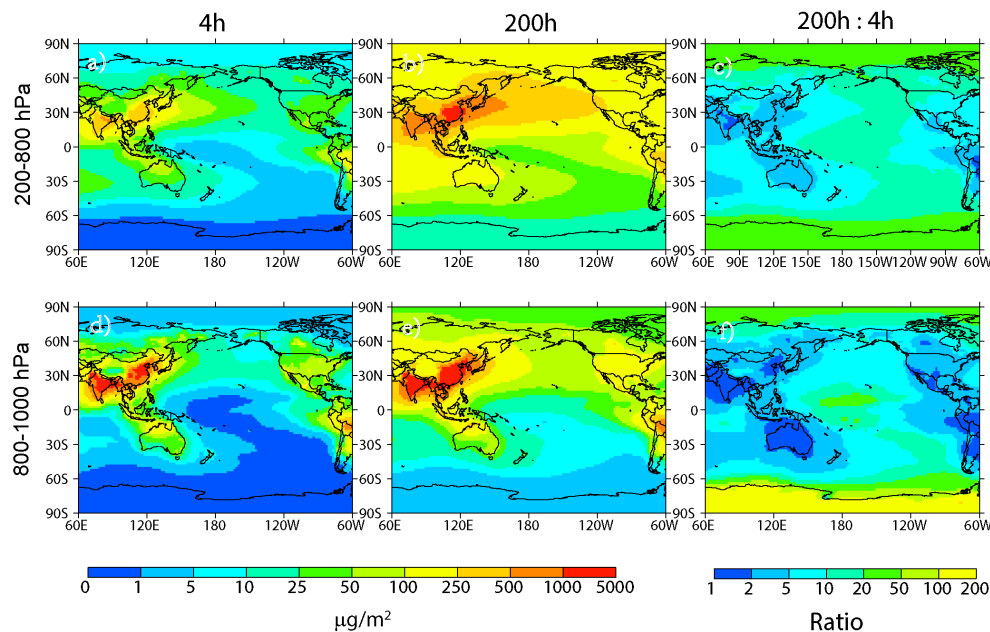


Figure 2. The annual averaged (2009–2011) column burden of BC at 200–800 hPa (**a, b**) and 800–1000 hPa (**d, e**) when aging timescale is 4 h (**a, d**) and 200 h (**b, e**). The ratio of BC burden for simulations with aging timescale of 200 h and 4 h is in Panels (**c**) and (**f**).

Title Page

Abstract

Introduction

Conclusions

References

Tables

Figures



Back

Close

Full Screen / Esc

Printer-friendly Version

Interactive Discussion



Long-range transport of black carbon to the Pacific Ocean

J. Zhang et al.

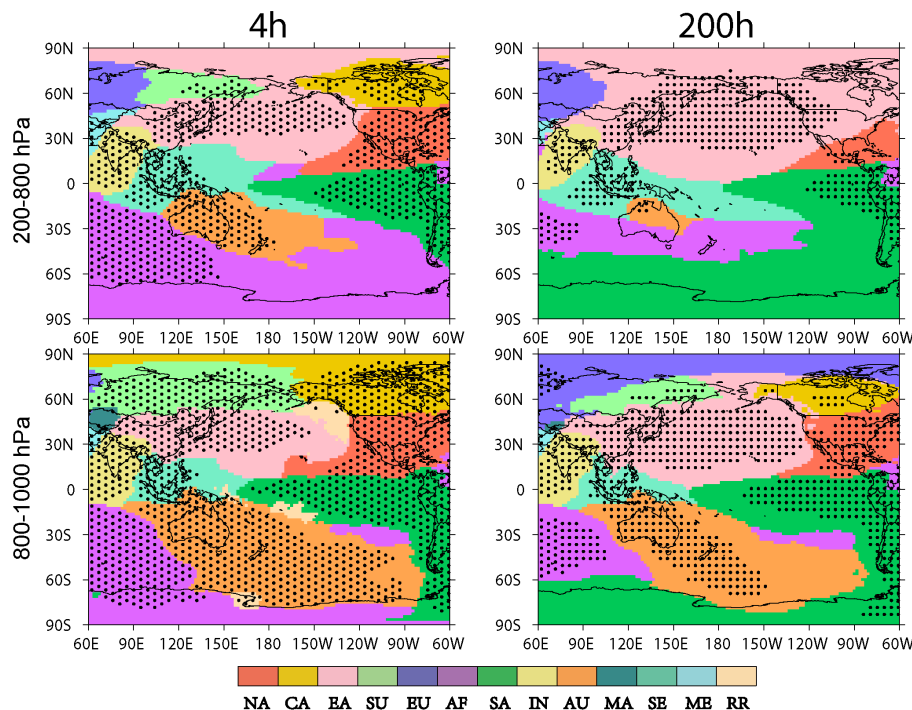


Figure 3. The dominant regional contributors to the annual averaged (2009–2011) column burden of BC at 200–800 hPa (top) and 800–1000 hPa (bottom) when aging timescale is 4 h (left) and 200 h (right). Dotted areas are where the dominant contributors account for more than 50 % of the total BC burden.

Title Page

Abstract

Introduction

Conclusions

References

Tables

Figures



Back

Close

Full Screen / Esc

Printer-friendly Version

Interactive Discussion



Long-range transport of black carbon to the Pacific Ocean

J. Zhang et al.

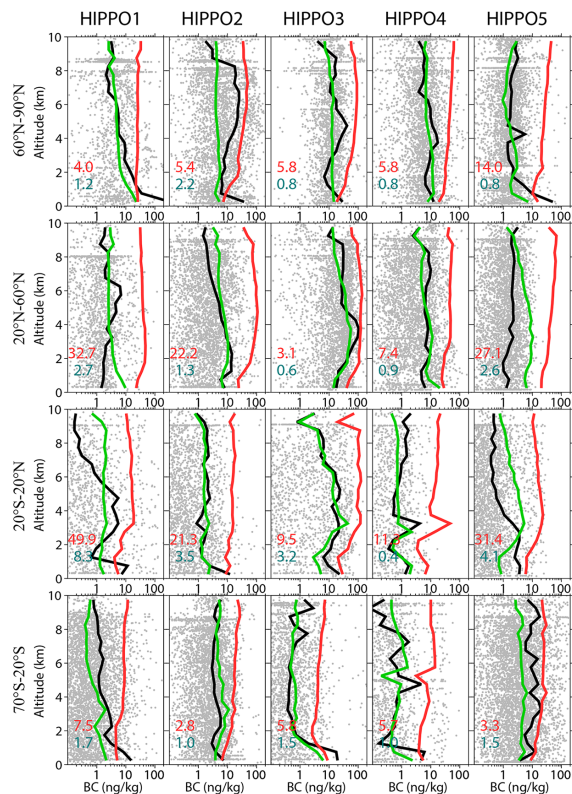


Figure 4. Vertical profiles of simulated and observed BC mass mixing ratios over 0.5 km altitude bins along the flight tracks of HIPPO 1–5 over the central Pacific Ocean (130° W–160° E). Data are shown separately as averaged over 70–20° S, 20° S–20° N, 20–60° N, and 60–90° N. The black, red, and green lines are mean values of BC mixing ratios from observations, default, and improved models, respectively. The gray dots represent measured BC concentrations. The green (red) number indicates the averaged NMAE for the improved (original) model (see Eq. 3).

Long-range transport of black carbon to the Pacific Ocean

J. Zhang et al.

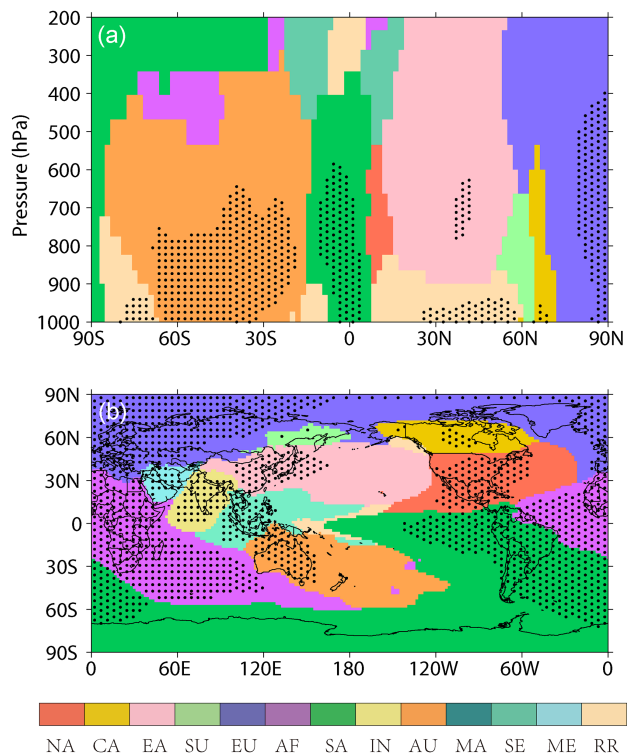


Figure 5. The most significant regional contributors to **(a)** zonal mean BC concentration over the Pacific (130° W–160° E), and **(b)** the column burden of BC in the troposphere (200–1000 hPa, 2009–2011 average). Dotted area represents where the most significant contributor accounts for more than 50% of the total BC.

Title Page

Abstract

Introduction

Conclusions

References

Tables

Figures

◀

▶

◀

▶

Back

Close

Full Screen / Esc

Printer-friendly Version

Interactive Discussion



